Influence of Al and Cu Doping on the Structure, Morphology, and Optical Properties of ZnO Thin Film

Faras Afifah[1,2], Arif Tjahjono[2], Aga Ridhova[3], Pramitha Yuniar Diah Maulida[4], Alfian Noviyanto[4,5*], and Didik Aryanto[1]**

[1]*Research Center for Advanced Materials, National Research and Innovation Agency, Kawasan Puspiptek Serpong, Tangerang Selatan, Banten 15314, Indonesia*

[2]*Department of Physics, Universitas Islam Negeri Syarif Hidayatullah, Jl. Ir. H. Juanda, Cempaka Putih, Jakarta 15412, Indonesia*

[3]*Research Center for Metallurgy and Materials, National Research and Innovation Agency, Kawasan Puspiptek Serpong, Tangerang Selatan, Banten 15314, Indonesia*

[4]*Nano Center Indonesia, Jl. Puspiptek, Tangerang Selatan, Banten 15314, Indonesia*

[5]*Department of Mechanical Engineering, Mercu Buana University, Jl. Meruya Selatan, Kebun Jeruk, Jakarta 11650, Indonesia*

Corresponding author:

email: a.noviyanto@nano.or.id; didi021@brin.go.id***

Received: February 23, 2022
Accepted: October 3, 2022

DOI: 10.22146/ijc.73234

Abstract: *In this study, ZnO thin films doped with Al (AZO) and Cu (CZO) were fabricated on a glass substrate via sol-gel spin coating. The influence of 1 atomic % Al and Cu doping on the structure, morphology, as well as optical properties of ZnO thin film was then analyzed with X-ray diffraction (XRD), atomic force microscopy (AFM), and UV-Vis spectroscopy. XRD analysis revealed that all samples possessed hexagonal wurtzite crystal structures with 3 to 4 preferred orientations. Al and Cu doping caused a decrease in crystal size, while the lattice strain (ε) and dislocation density (ρ) were increased. AFM indicated that Al and Cu doping reduced the surface roughness of the ZnO thin film. Optical measurement showed that all samples exhibited high transmittance (> 80%) in the visible light region. Transmittance was reduced after doping, while the band gaps for ZnO, AZO, and CZO thin films are 3.26, 3.28, and 3.23 eV. This study showed that an addition of 1 atomic % transition metal (Al and Cu) greatly influences the structure, morphology, and optical properties of ZnO thin film.*

Keywords: *doping; morphology; optical properties; structure; thin film*

■ INTRODUCTION

Zinc oxide (ZnO) is a semiconductor II-VI with a bandgap of 3.2-3.3 eV and a strong excitation binding energy (60 MeV) at room temperature [1-3]. ZnO is a polycrystalline material and could exist in wurtzite, zinc-blende, and cubic rock salt form, with wurtzite being the most abundant due to it being the most stable [4]. In addition, ZnO is known to be non-toxic, eco-friendly, easy to process, and possesses high chemical stability [1-2,5-8]. In thin-film form, ZnO has high optical transmittance, high electron mobility, and thermal conductivity [9-10]. These properties make ZnO suitable for many applications, such as solar cells [11], transparent conductive oxide (TCO) [12], light-emitting diode [13], and photocatalysts [6,14]. Therefore, various improvements in ZnO thin film have been the subject of much research.

The doping process is a promising way to modify the microstructure and both optical and electronic properties of ZnO. Some studies have reported that elements from the III group (Al, In, Ga) [5,7,15] and transition metals (Ti, V, Cr, Mn, Fe, Co, Ni, Cu) [10,16-17] are suitable dopant candidates for ZnO thin film. A previous study by Asikuzun et al. showed that doping ZnO thin film with Cu increased the surface roughness, lowered the optical transmittance, and lowered the optical band gap [18]. A similar result was reported by

Nimbalkar and Patil [13], who confirmed that the band gap, as well as the activation energy of ZnO thin film, were decreased after Cu doping.

On the other hand, Al doping has been reported to lower the crystal quality and band gap of ZnO thin film. However, lattice strain and Seebeck coefficient were conserved [19]. Another study found that band gap, lattice parameter, and grain size decreased after Al was added [20]. According to the studies mentioned earlier, the addition of Al and Cu could affect the morphology and optical properties of ZnO thin film.

From the chemical and physical perspectives, Cu is a more suitable candidate as a dopant for ZnO, as Cu has similar atomic properties to Zn, particularly in terms of atomic radius and electron shell [18]. The substitution of Cu^{2+} into Zn^{2+} is thought not to cause a notable change in lattice parameters, seeing as the radii of Cu^{2+} and Zn^{2+} are estimated to be around 0.073 and 0.074 nm [21]. In contrast, Al with an ionic radius of 0.053 nm is expected to cause a significant alteration in the lattice parameter, owing to the large radius difference. A previous study of Al- and/or Cu- doped ZnO thin film has been conducted [11-14,18-19,21-28]. However, the investigation focuses on the effect of only one doping (Al or Cu) in the ZnO thin film. Bakhtiargobandi et al. [29] investigated the effect of Al and Cu doping on the photoelectrochemical properties of ZnO thin films, nevertheless, the amount of dopants is large, i.e., 6 wt.%. To the best of our knowledge, there has been no report on the small number of dopants (Cu and Al) on the structure, morphology, and optical properties of ZnO thin films. The addition of small doping with different ionic radii on the structure, morphology and optical properties of ZnO becomes the focus of the present study, where ion radii of Cu are closer to that of Zn compared to ion radii of Al. In general, the least amount of reported doping of Cu or Al on ZnO is 1 atomic %. The interesting finding is that it has an effect on the properties of the thin films, especially with the addition of two different dopant atomic radii with Zn.

In this research, ZnO thin film was doped with Al and Cu, each with a concentration of 1%. The thin films were deposited onto a glass substrate using a sol-gel spin coating. This method was used due to its being safe, easy to operate, and low cost [1-2] when compared to other methods such as pulsed laser deposition (PLD), chemical vapor deposition (CVD), sputtering [7], spray pyrolysis [21], chemical bath deposition, electrochemical deposition, and hydrothermal [13]. The influence of 1% Al and Cu doping on ZnO thin film's morphology, structure, and optical properties were evaluated thoroughly using X-ray diffraction (XRD), atomic force microscopy (AFM), and UV-Vis spectroscopy.

■ EXPERIMENTAL SECTION

Materials

The materials used in this research were zinc acetate dihydrate ($Zn(CH_3COO)_2{\cdot}2H_2O$) (CAS number 5970-45-6, Merck KGaA), isopropanol (CAS number 67-63-0, Merck KGaA), ethanolamine ($NH_2CH_2CH_2OH$) (CAS number 141-43-5, Merck KGaA), Copper(II) acetate monohydrate ($Cu(CH_3COO)_2{\cdot}H_2O$) (CAS number 6046-93-1, Merck KGaA), and aluminum acetate ($C_4H_7AlO_5$) (CAS number 142-03-0, Sigma-Aldrich) were used in this study.

Instrumentation

VTC-100 spin coater was used to fabricate the thin film. Phase analysis was conducted by X-ray diffraction (XRD, Smartlab, Rigaku, Japan). The surface roughness of samples was observed by atomic force microscopy (AFM, NX10 AFM, Korea). The band gap of the sample was obtained from UV-Vis spectroscopy (UH5300, Hitachi, Japan).

Procedure

Copper(II) acetate monohydrate ($Cu(CH_3COO)_2{\cdot}H_2O$) and aluminum acetate ($C_4H_7AlO_5$) was added into the solution to make Cu-doped (CZO) and Al-doped (AZO) ZnO thin film, respectively. The percentage of dopants was calculated according to the molecular weight of the dopants.

Both ZnO and dopant precursor solution has a concentration of 0.5 M with the molar ratio of metal salt and ethanolamine 1:1. Undoped and doped ZnO solution were stirred at a temperature of 60 °C for 1 h with 300 rpm and was left at room temperature for 24 h.

Glass substrates were cleaned using the radio corporation of America (RCA) method, where the substrates were cleaned with ethanol for 10 min and acetone for 5 min using an ultrasonic cleaner to ensure that no organic impurities remained in the sample. The substrates were then rinsed with deionized water.

The solutions were deposited into the substrates using spin-coating (3000 rpm for 50 s) using VTC-100 spin coater to fabricate the thin films. The deposition process was repeated three times, with a pre-heated treatment at a temperature of 110 °C for 10 min. The final heat treatment for the ZnO thin film was done at 400 °C for 1 h.

■ RESULTS AND DISCUSSION

Fig. 1 shows the diffraction pattern of ZnO, AZO, and CZO deposited using sol-gel spin coating. According to ICDD [96-230-0113], all samples have a hexagonal wurtzite structure. Crystal growth and orientation of each sample could be further analyzed using the texture coefficient (TC) obtained from the Harris equation, as shown in Eq. (1).

$$TC = \frac{I_{(hkl)} / I_{0(hkl)}}{\left(1/n \sum I_{(hkl)} / I_{0(hkl)} \right)} \quad (1)$$

where n, $I_{(hkl)}$, and $I_{0(hkl)}$ represent the number of diffraction peaks, peak intensity of a certain plane, and reference intensity. Calculated TC of ZnO, AZO, and CZO, along with the planes associated with diffraction peaks, are presented in Table 1. According to TC calculation, each sample tends to crystallize in a different orientation, as the crystal growth could be attributed to a few particular planes. ZnO tends to crystallize in the direction of (002), (101), and (112) planes. Crystal growth in AZO is dominated by (102), (110), and (112) planes, while CZO crystallization mostly occurs in (100), (101), (110), and (112) orientations.

The incorporation of Cu and Al also caused the peak intensity of ZnO to decrease, although the decrease is more significant in AZO. This is due to the large difference in ionic radii between Al and Zn, while the ionic radii of Cu and Zn only while the difference in ionic radii for Cu and Zn insignificant. The atomic radii of Al^{3+}, Cu^{2+}, and Zn^{2+} are 0.053, 0.073, and 0.074 nm, respectively. The immense difference between Al and Zn atomic radii would result in a more notable distortion in the ZnO crystal structure, hence the less crystalline structure of AZO [17].

Additionally, other properties are also affected by the doping process, such as lattice parameters (a and c), crystal size (D), lattice strain (ε), and dislocation density (ρ). Lattice parameters (a and c) and *d*-spacing (d) of each

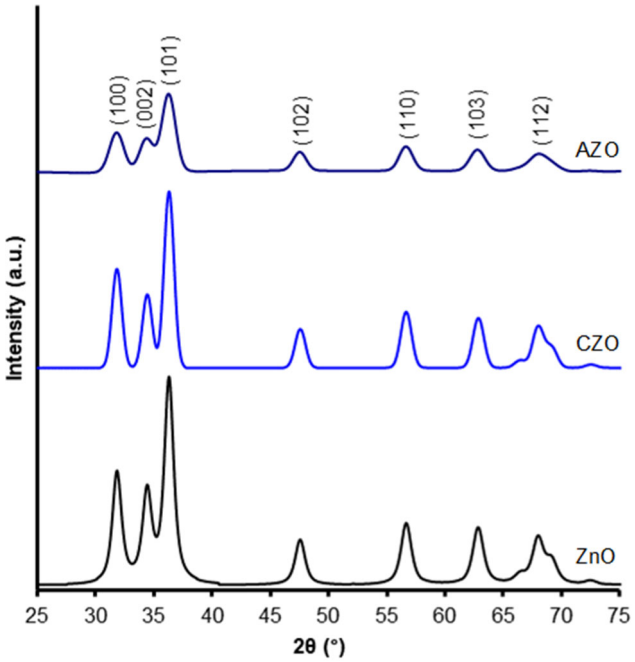

Fig 1. Diffraction pattern of ZnO, AZO, and CZO thin film

Table 1. Texture coefficient (TC) of ZnO, AZO, and CZO thin film

Sample	Texture Coefficient (TC)						
	(100)	(002)	(101)	(102)	(110)	(103)	(112)
ZnO	0.97	1.11	1.01	0.95	0.94	0.97	1.05
CZO	1.00	0.96	1.02	0.97	1.01	0.99	1.06
AZO	0.88	0.98	0.98	1.13	1.02	0.99	1.03

sample could be evaluated using the following relations, according to Eq. (2-4), respectively.

$$a = \frac{\lambda}{\sqrt{3}\sin\theta}\sqrt{h^2 + hk + k^2} \quad (2)$$

$$c = \frac{\lambda}{2\sin\theta}l \quad (3)$$

$$\frac{1}{d^2} = \frac{4\sin^2\theta}{\lambda^2} \quad (4)$$

where λ is the X-ray wavelength (1.5405 Å), θ is the diffraction angle, and h k l are the Miller indices.

Crystal size (D) could be calculated using the Debye-Scherrer formula, as shown in Eq. (5).

$$D = \frac{0.94\lambda}{B\cos\theta} \quad (5)$$

where B represents the full width at half maximum (FWHM) of a particular peak (h k l).

Lattice strain (ε), which is a lattice disorder developed during crystallization, could be calculated using the following Eq. (6).

$$\varepsilon = \frac{B}{4\tan\theta} \quad (6)$$

Dislocation density (ρ) is defined as dislocation-induced imperfection present in a unit volume and could be calculated using the Williamson-Smallman relation (Eq. (7)).

$$\rho = \frac{1}{D^2} \quad (7)$$

Table 2 shows the calculated crystallography parameter such as lattice parameter, crystal size (D), d-spacing (d), lattice strain (ε), and dislocation density (ρ) of ZnO, AZO, and CZO. Al doping resulted in a decrease in lattice constant, while Cu doping increased. The change in lattice parameter is related to the addition of Al and Cu. A similar result has been reported by Jongnavakit et al., where ZnO underwent a decrease in lattice constant after Cu doping [30]. Al Farsi et al. also reported that Al doping caused the lattice constant of thin film to increase [22].

A shift in lattice constant also indicates an alteration in crystal size (D), where the crystal size of ZnO, AZO, and CZO calculated from the (112) plane are 50.48, 38.38, and 47.96 nm, respectively. This change in crystal size is clearly observed in the broadening of the peak, as shown in Fig. 1, which shows that the addition of Al caused the peak to broaden; thus, the crystallite size decreased compared to ZnO. These changes also show that the doping process was successful, as evidenced by the decrease in crystal size in both doped samples. Moreover, studies by de Lara Andrade et al. and Ali et al. demonstrate that ZnO crystal size decreased along with the increase of Al^{3+} and Cu^{2+} concentrations [23-24]. The ionic radii of the dopants also affect the d-spacing, which represents the distance between parallel planes in the structure. AZO and CZO have lower *d*-spacing than ZnO, where the calculated values are 1.3772, 1.3781, and 1.3784, respectively. Similar to crystal size, AZO has the lowest *d*-spacing value as a consequence of the small ionic radius of Al^{3+}.

Furthermore, immense atomic radii differences would consequently cause higher lattice strain in the ZnO structure. Higher lattice strain would result in more dislocation and therefore cause the structure to have a higher dislocation density, as observed in both samples, particularly AZO, which exhibits a significantly higher dislocation density than CZO and ZnO. Additionally, there are published reports that Al and Cu doping increased the lattice strain, which led to an increase in defects in grain boundaries, reinforcing that higher lattice strain is related to higher dislocation in a crystal structure [19,24]. Another suggestion is that the addition of Al and

Table 2. Lattice parameter, crystal size (D), *d*-spacing (d), lattice strain (ε), and dislocation density (ρ) calculated from plane (112)

Sample	a (Å)	c (Å)	D (Å)	d (Å)	ε (%)	ρ (× 10^{-2}) (line/nm^2)
ZnO	3.2473	5.2111	50.48	1.3784	1.229	3.92
CZO	3.2473	5.2097	47.96	1.3781	1.293	4.34
AZO	3.2503	5.2170	38.38	1.3772	1.615	6.79

Cu could inhibit crystal growth, in which case the lattice distortion is bound to occur [24].

Fig. 2 represents the three-dimensional 2 × 2 µm surface topology of ZnO, AZO, and CZO thin film obtained from AFM analysis. Visually, it could be observed that the addition of Al and Cu to ZnO reshaped its surface topology, as indicated by the relatively more even surface of AZO and CZO. The morphology parameter was further analyzed using Gwyddion software, from which grain size, average surface roughness, and root mean square surface roughness were obtained and presented in Table 3.

The average grain size ranged from 29.95 to 51.95 nm, as shown in Table 3. After being doped with Al, the grain size of the ZnO thin film was reduced from 36.68 to 29.95 nm. Previous studies by Al Farsi et al. and Hsu et al. also found that Al doping resulted in a decrease in grain size and surface roughness [22,25]. The opposite could be observed in Cu doping, where the grain size increased to 51.95 nm. This result is also in agreement with a study by Istrate et al., who found that the addition of Cu increased the grain size of ZnO thin film [26].

In addition to grain size, the surface topology of each sample is also related to its surface roughness, which was determined by the distribution of its grain. In ZnO, the surface is riddled with elliptical grains of varying sizes, while in AZO and CZO, the grains are more homogenous and evenly distributed. As a result, the average surface roughness of Cu-doped ZnO is slightly lower than that of pristine ZnO, while in Al-doped ZnO, the roughness is reduced to almost a quarter of its initial. On top of that, root mean square (RMS) roughness analysis yields a similar result, which further confirms that the grain of AZO is finer and notably more homogenous than CZO and ZnO.

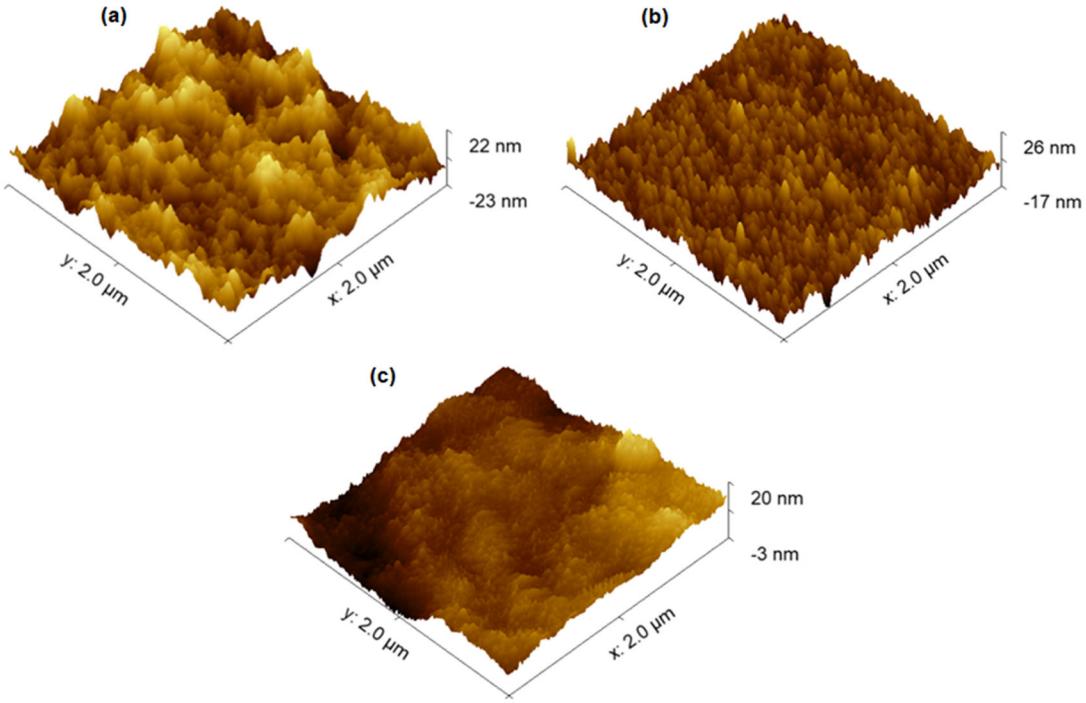

Fig 2. AFM images of (a) ZnO, (b) CZO, and (c) AZO thin film

Table 3. Grain size, average roughness, and RMS roughness of ZnO, AZO, and CZO thin film

Sample	Grain size (nm)	Average roughness (nm)	RMS roughness (nm)
ZnO	36.68	2.02	2.59
CZO	51.95	1.93	2.45
AZO	29.95	0.54	0.69

Fig. 3 shows the optical transmittance of ZnO, AZO, and CZO within the wavelength ranging from 200–1000 nm. Generally, all samples exhibit around 80–90% transmittance in the visible light region. This property is particularly useful for optoelectronics applications such as a transparent electrodes in solar cells. However, the transmittance of AZO and CZO in the visible light region was lower. This could be explained using the structure disorder caused by the incorporation of dopants. After the doping process, ZnO has a higher amount of structural disorder. These defects would increase the optical scattering of ZnO so that the doped samples will have lower transmittance than pristine ZnO. Since structural defects contribute to optical scattering, a higher concentration of defects in a structure indicates poor optical transmittance [18]. This result also agrees with the XRD data, where AZO with the highest amount of disorder in its structure has the lowest transmittance among other samples.

Fig. 3 also reveals the blue shift in both AZO and CZO, where the absorption edge shifted toward a shorter wavelength. After Al doping, the edge shifted from 360 to 300 nm, while Cu doping caused it to shift to 320 nm. This shift would later play a role in determining the bandgap and evaluating the charge carrier concentration. These findings are in agreement with studies related to absorption edge shift in ZnO thin film after Al doping [31] and Cu doping [30].

From transmittance data, the optical band gap could be calculated by using Eq. (8).

$$(\alpha h\nu)^2 = B(h\nu - E_g) \quad (8)$$

where α is the absorption coefficient, B is the edge width parameter, hν is the photon energy, and n = 2 (for semiconductor band gap). The absorption coefficient (α) of the thin film samples could be obtained by using this relation (9).

$$\alpha = \frac{1}{t}\ln\left(\frac{1}{T}\right) \quad (9)$$

in which t is the thickness of the thin film. Thin-film bandgap could be acquired from the linear extrapolation of $(\alpha h\nu)^2$ with hν.

As shown in Fig. 4, the optical band gaps of ZnO, AZO, and CZO thin films are 3.26, 3.28, and 3.23 eV. In the thin film, ZnO has a lower band gap than bulk ZnO (3.37 eV). The lower value is due to the heat treatment and the structural defects formed during the fabrication process [19]. For doped samples, Al doping increased the optical band gap of ZnO, while Cu doping lowered the band gap. The shifting of the band gap in ZnO thin film doped with transition metal could be explained by the Burstein-Moss effect. Al^{3+} and Cu^{2+} ions introduced charge carriers into ZnO, which would then modify the band gap.

In AZO, the Al atom, which has more valence electrons than Zn, would introduce more charge carrier concentration in the ZnO thin film. These carriers would

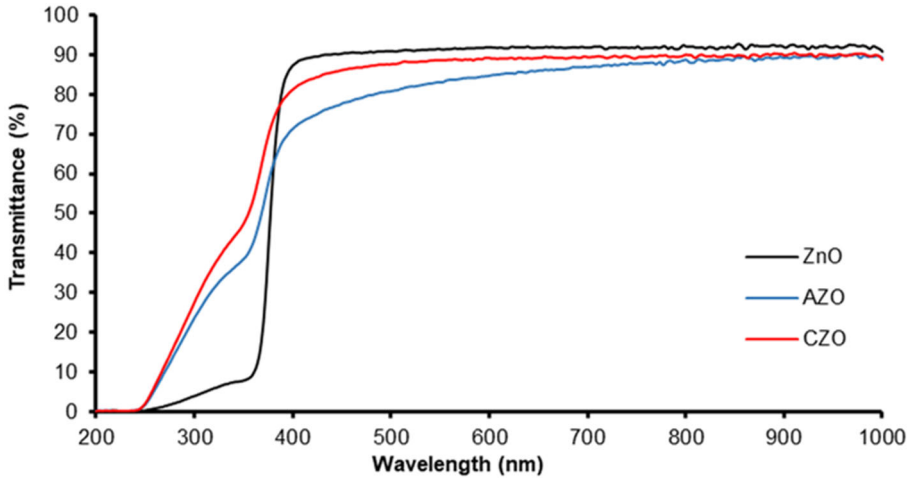

Fig 3. Optical transmittance of ZnO, AZO, and CZO thin film

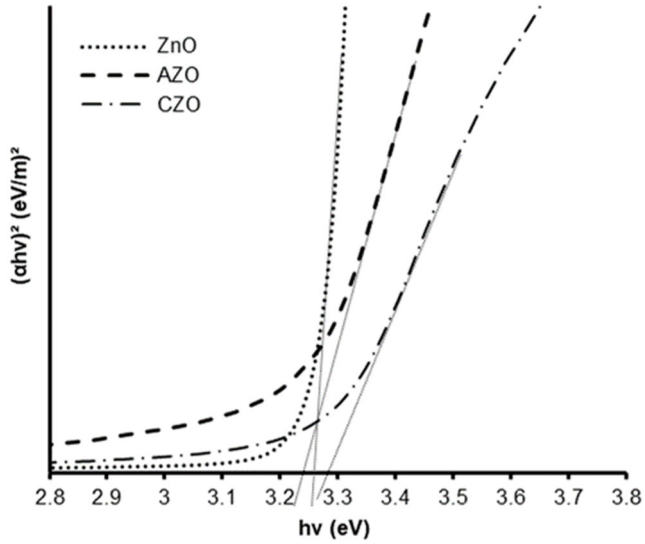

Fig 4. Optical band gap of ZnO, AZO, and CZO

create sites near the conduction band, which would consequently draw the Fermi energy closer to the conduction band, thus increasing the band gap [28]. This also explains the blue shift in absorption edge, where the shift toward a lower wavelength suggests that it would require higher energy to induce a photocatalytic effect in AZO. Likewise, the Cu atom in CZO would create more sites near the valence band and lower the band gap. The band gap shift also proves that the doping process was successful. Additionally, Bakhtiargonbadi et al. suggested that $Cu_{Zn}^{\bullet}$ donor-acceptor played a role in lowering the ZnO bandgap, along with $V_O^{\bullet\bullet}$, $V_{Zn}^{\bullet\bullet}$ and $Zn_i^{\bullet\bullet}$ [29].

■ CONCLUSION

ZnO thin films doped with 1% Al and Cu were fabricated using sol-gel spin coating, and the structure, morphology, and optical properties of the thin films were then analyzed. The diffraction pattern of thin films confirmed the structure of hexagonal wurtzite. Texture coefficient calculation showed that each sample tends to crystallize in a different orientation, particularly during heat treatment. Al and Cu doping resulted in lowered crystal size (D), average surface roughness, and transmittance, as well as heightened lattice strain (ε) and dislocation density (ρ). Moreover, shifts in band gaps have been observed according to the type of dopants. ZnO, AZO, and CZO have band gap values of 3.26, 3.28, and 3.23 eV, respectively. In conclusion, the slight addition of 1 atomic % transition metal (Al and Cu) proved to greatly influence the structure, morphology, and optical properties of ZnO thin film.

■ ACKNOWLEDGMENTS

No funding was used to support this research. We thank Research Center for Advanced Materials-BRIN for the facilities and characterization.

■ AUTHOR CONTRIBUTIONS

Faras Afifah: Writing the original draft and conducted the experiment. Arif Tjahjono: Formal analysis, supervision. Aga Ridhova: Conducted the AFM characterization. Pramitha Yuniar Diah Maulida: Formal analysis. Alfian Noviyanto: formal analysis, visualization, writing - review & editing. Didik Aryanto: Conceptualization, methodology, conducted the experiment, formal analysis, visualization, supervision, writing - review & editing.

■ REFERENCES

[1] Aryanto, D., Maulana, R.M., Sudiro, T., Masturi, M., Wismogroho, A.S., Sebayang, P., Ginting, M., and Marwoto, P., 2017, Effect of post-thermal annealing on the structural of ZnO thin films deposited using sol-gel spin-coating method, *AIP Conf. Proc.*, 1862, 030045.

[2] Aryanto, D., Jannah, W.N., Masturi, M., Sudiro, T., Wismogroho, A.S., Sebayang, P., Sugianto, S., and Marwoto, P., 2017, Preparation and structural characterization of ZnO thin films by sol-gel method, *J. Phys.: Conf. Ser.*, 755, 012025.

[3] Giri, P., and Chakrabarti, P., 2016, Effect of Mg doping in ZnO buffer layer on ZnO thin film devices for electronic applications, *Superlattices Microstruct.*, 93, 248–260.

[4] Sirelkhatim, A., Mahmud, S., Seeni, A., Mohamad Kaus, N.H., Ann, L.C., Mohd Bakhori, S.K., Hasan, H., and Mohamad, D., 2015, Review on zinc oxide nanoparticles: Antibacterial activity and toxicity mechanism, *Nano-Micro Lett.*, 7 (3), 219–242.

[5] Aryanto, D., Marwoto, P., Sudiro, T., Wismogroho, A.S., and Sugianto, S., 2019, Growth of a-axis-oriented Al-doped ZnO thin film on glass substrate

using unbalanced DC magnetron sputtering, *J. Phys.: Conf. Ser.*, 1191, 012031.

[6] Aryanto, D., Hastuti, E., Taspika, M., Anam, K., Isnaeni, I., Widayatno, W.B., Wismogroho, A.S., Marwoto, P., Nuryadin, B.W., Noviyanto, A., and Sugianto, S., 2020, Characteristics and photocatalytic activity of highly *c*-axis-oriented ZnO thin films, *J. Sol-Gel Sci. Technol.*, 96 (1), 226–235.

[7] Nulhakim, L., Makino, H., Kishimoto, S., Nomoto, J., and Yamamoto, T., 2017, Enhancement of the hydrogen gas sensitivity by large distribution of c-axis preferred orientation in highly Ga-doped ZnO polycrystalline thin films, *Mater. Sci. Semicond. Process.*, 68, 322–326.

[8] Yathisha, R.O., and Nayaka, Y.A., 2020, Effect of solvents on structural, optical and electrical properties of ZnO nanoparticles synthesized by microwave heating route, *Inorg. Chem. Commun.*, 115, 107877.

[9] Zhang, W., Gan, J., Li, L., Hu, Z., Shi, L., Xu, N., Sun, J., and Wu, J., 2018, Tailoring of optical and electrical properties of transparent and conductive Al-doped ZnO films by adjustment of Al concentration, *Mater. Sci. Semicond. Process.*, 74, 147–153.

[10] Sahoo, B., Pradhan, S.K., Mishra, D.K., Sahoo, S.K., Nayak, R.R., and Behera, D., 2021, Mutual effect of solvent and Fe-In codoping on structural, optical and electronic properties of ZnO thin films prepared by spray pyrolysis technique, *Optik*, 228, 166134.

[11] Ge, Z., Wang, C., Chen, T., Chen, Z., Wang, T., Guo, L., Qi, G., and Liu, J., 2020, Preparation of Cu-doped ZnO nanoparticles via layered double hydroxide and application for dye-sensitized solar cells, *J. Phys. Chem. Solids*, 150, 109833.

[12] Ou, S.L., Lai, F.M., Yuan, L.W., Cheng, D.L., and Kao, K.S., 2016, Characterization of Al-doped ZnO transparent conducting thin film prepared by off-axis magnetron sputtering, *J. Nanomater.*, 2016, 6250640.

[13] Nimbalkar, A., and Patil, M., 2017, Synthesis of highly selective and sensitive Cu-doped ZnO thin film sensor for detection of H_2S gas, *Mater. Sci. Semicond. Process.*, 71, 332–341.

[14] Alatawi, N.M., Saad, L.B., Soltane, L., Moulahi, A., Mjejri, I., and Sediri, F., 2021, Enhanced solar photocatalytic performance of Cu-doped nanosized ZnO, *Polyhedron*, 197, 115022.

[15] Marwoto, P., Wibowo, E., Suprayogi, D., Sulhadi, S., Aryanto, D., and Sugianto, S., 2016, Properties of ZnO:Ga thin films deposited by dc magnetron sputtering: Influence of Ga-doped concentrations on structural and optical properties, *Am. J. Appl. Sci.*, 13 (12), 1394–1399.

[16] Aryanto, D., Hastuti, E., Husniya, N., Sudiro, T., and Nuryadin, B.W., 2018, Synthesis, characterization, and photocatalytic properties of nanocrystalline NZO thin films, *J. Phys.: Conf. Ser.*, 985, 012025.

[17] Koresh, I., and Amouyal, Y., 2017, Effects of microstructure evolution on transport properties of thermoelectric nickel-doped zinc oxide, *J. Eur. Ceram. Soc.*, 37 (11), 3541–3550.

[18] Asikuzun, E., Ozturk, O., Arda, L., and Terzioglu, C., 2018, Preparation, growth and characterization of nonvacuum Cu-doped ZnO thin films, *J. Mol. Struct.*, 1165, 1–7.

[19] Ambedkar, A.K., Singh, M., Kumar, V., Kumar, V., Singh, B.P., Kumar, A., and Gautam, Y.K., 2020, Structural, optical and thermoelectric properties of Al-doped ZnO thin films prepared by spray pyrolysis, *Surf. Interfaces*, 19, 100504.

[20] Kathwate, L.H., Umadevi, G., Kulal, P.M., Nagaraju, P., Dubal, D.P., Nanjundan, A.K., and Mote, V.D., 2020, Ammonia gas sensing properties of Al doped ZnO thin films, *Sens. Actuators, A*, 313, 112193.

[21] Wang, D., Zhou, J., and Liu, G., 2009, The microstructure and photoluminescence of Cu-doped ZnO nano-crystal thin films prepared by sol-gel method, *J. Alloys Compd.*, 487 (1-2), 545–549.

[22] Al Farsi, B., Souier, T.M., Al Marzouqi, F., Al Maashani, M., Bououdina, M., Widatallah, H.M., and Al Abri, M., 2021, Structural and optical properties of visible active photocatalytic Al doped ZnO nanostructured thin films prepared by dip coating, *Opt. Mater.*, 113, 110868.

[23] de Lara Andrade, J., Oliveira, A.G., Mariucci, V.V.G., Bento, A.C., Companhoni, M.V., Nakamura, C.V., Lima, S.M., da Cunha Andrade, L.H., Moraes, J.C.G., Hechenleitner, A.A.W., Pineda, E.A.G., and de Oliveira, D.M.F., 2017, Effects of Al^{3+} concentration on the optical, structural, photocatalytic and cytotoxic properties of Al-doped ZnO, *J. Alloys Compd.*, 729, 978–987.

[24] Ali, G.A., Emam-Ismail, M., El-Hagary, M., Shaaban, E.R., Moustafa, S.H., Amer, M.I., and Shaban, H., 2021, Optical and microstructural characterization of nanocrystalline Cu doped ZnO diluted magnetic semiconductor thin film for optoelectronic applications, *Opt. Mater.*, 119, 111312.

[25] Hsu, C.H., Geng, X.P., Huang, P.H., Wu, W.Y., Zhao, M.J., Zhang, X.Y., Huang, Q.H., Su, Z.B., Chen, Z.R., Lien, S.Y., and Zhu, W.Z., 2021, High doping efficiency Al-doped ZnO films prepared by co-injection spatial atomic layer deposition, *J. Alloys Compd.*, 884, 161025.

[26] Istrate, A.I., Mihalache, I., Romanitan, C., Tutunaru, O., Gavrila, R., and Dediu, V., 2021, Copper doping effect on the properties in ZnO films deposited by sol–gel, *J. Mater. Sci.: Mater. Electron.*, 32 (4), 4021–4033.

[27] Hong, M.H., Choi, H., Shim, D.I., Cho, H.H., Kim, J., and Park, H.H., 2018, Study of the effect of stress/strain of mesoporous Al-doped ZnO thin films on thermoelectric properties, *Solid State Sci.*, 82, 84–91.

[28] Mondal, S., Bhattacharyya, S.R., and Mitra, P., 2013, Effect of Al doping on microstructure and optical band gap of ZnO thin film synthesized by successive ion layer adsorption and reaction, *Pramana*, 80 (2), 315–326.

[29] Bakhtiargonbadi, F., Esfahani, H., Moakhar, R.S., and Dabir, F., 2020, Fabrication of novel electrospun Al and Cu doped ZnO thin films and evaluation of photoelectrical and sunlight-driven photoelectrochemical properties, *Mater. Chem. Phys.*, 252, 123270.

[30] Jongnavakit, P., Amornpitoksuk, P., Suwanboon, S., and Ndiege, N., 2012, Preparation and photocatalytic activity of Cu-doped ZnO thin films prepared by the sol-gel method, *Appl. Surf. Sci.*, 258 (20), 8192–8198.

[31] Yang, S., Gu, H., and Huang, A., 2021, Effect of oxygen partial pressure on microstructure, optical and electrical property of C-Al co-doped ZnO films, *Mater. Sci. Semicond. Process.*, 133, 105946.